RESEARCH ARTICLE

Journal of Medical Imaging and Health Informatics
Vol. 4, 1–7, 2014

Classification of Breast Tissue as Normal or Abnormal Based on Texture Analysis of Digital Mammogram

Fatehia B. Garma and Mawia A. Hassan*

Biomedical Engineering Department, Sudan University of Science and Technology, Khartoum, Sudan

The breast cancer is a serious public health problem among women in the world. Efforts in Computer Vision have been made in order to improve the diagnostic accuracy by radiologists. In this paper a method for detection of breast cancer based on digital mammogram analysis was presented. Haralick texture features were derived from spatial grey level dependency (SGLD) matrix. The features were extracted from each Region of interest (ROIs). The features discriminating to detect abnormal from normal tissues were determined by stepwise linear discriminant analysis classifier. The proposed method achieved 95.7% of relative accuracy for classification of breast tissues based on digital mammogram texture analysis.

Keywords: Breast Cancer, Mammogram Image, Texture Analysis, Haralick Texture Features, Linear Discrimination Analysis.

1. INTRODUCTION

Breast cancer is a type of cancer originating from breast tissue. It is the most public health problem among women. If breast cancer is detected early; the treatment can be performed earlier and therefore be more efficient. Mammography is the most common technique for early detection of breast cancer. It is considered the most effective, low cost, and reliable technique for early detection of this disease.[1]

With the advances of digital image processing, radiologists have a chance to improve their performance with computer-aided detection and diagnosis (CAD) system; this technology can be used with standard film mammograms or with digital mammograms.[2]

Breast Cancer cells can be of different types and shapes.[19] The presence of other structures makes the mammogram background very complex for physician to distinguish malignant mass lesions from normal breast tissues.[12] Also, the sensitivity of mammographic screening varies with image quality and expertise of the radiologist.[20] That leads to misinterpretation of mammograms, and to reduce the high misinterpretation rate, an objective method to classify and identify the pathology on the mammogram is needed.[21]

One method to identify the breast cancer is texture analysis in mammogram. Textures are one of the important characteristics for identifying objects and ROI of various images.[3] Texture analysis is important for application of computer image analysis for classification, detection and segmentation of an image based on intensity and colour.[4]

2. PREVIOUS METHODS

Several papers addressed the issues involved to detect and classify the breast cancer in digital mammograms. Chan et al.[2] classified breast tissue on mammograms into masses and normal using texture features derived from SGLD matrix and stepwise linear discriminant analysis to perform classification. The classifier achieved an average area (Az) under the receiver operating characteristics (ROC) curve, $Az = 0.84$ during training and 0.82 during testing. Wang and Karayiannis[5] were presented an approach for detecting microcalcifications in digital mammograms using wavelet-based sub-band image decomposition, and then reconstructing the mammogram from the sub-bands containing only high frequencies. The reconstructed mammogram is expected to contain only high-frequency components, including the microcalcifications. Sheshadri and Kandaswamy[6] studied breast tissue classification using statistic feature extraction of mammography. The statistical features extracted are the mean, standard deviation, smoothness, third moment, uniformity and entropy which signify the important texture features of breast tissue. Classify the breast tissue into four basic categories like fatty, uncompressed fatty, dense and high density. The Accuracy of the proposed method has been verified with the ground truth given in the data base (mini-MIAS database) and has

*Author to whom correspondence should be addressed.

obtained accuracy as high as 78%. Martins et al.[7] presented a methodology for masses detection on digitized mammograms using the K-means algorithm for image segmentation and co-occurrence matrix to describe the texture of segmented structures. Classification of these structures is accomplished through Support Vector Machines, which separate them in two groups, using shape and texture descriptors: masses and non-masses. The methodology obtained 85% of accuracy. Mohd. Khuzi et al.[8] classified ROI in digital mammogram as either masses and non-masses tissues by using local threshold, K mean clustering and Otsu's methods for segmentation of the ROI and SGLD matrix resulting in ROC curve area of $Az = 0.84$ for Otsu's method, 0.82 for thresholding method and $Az = 0.7$ for K-mean clustering. ROC curve area of 0.8–0.9 is rated as good result. Gorgel et al.[9] investigated an approach for classification of mammographic masses as benign or malign. Decision making was performed in two stages as feature extraction by computing the wavelet coefficients and classification using the classifier trained on the extracted Features using Support Vector Machine (SVM). The research involved 66 digitized mammographic images. The masses were segmented manually by radiologists, prior to introduction to the classification system. Preliminary test on mammogram showed over 84.8% classification accuracy by using the SVM with Radial Basis Function (RBF) kernel. Rajkumar and Raju[10] presented a comparative study of performance of discrete wavelet transformation and stationary wavelet transformation for classifying mammogram images into Normal, Benign and Malignant. In each wavelet transformations, a fractional part of the highest wavelet coefficients is used as features for classification. Using discrete wavelet transformation achieved 83% of the images classified correctly. On the other hand using stationary wavelet transformation obtained only 76% of accuracy. The study also reveals that the redundant nature of coefficients in stationary wavelet transformation is not suitable for identifying tumors in mammograms. Dehghani and Dezfooli[11] designed and complemented a system for diagnosis and classification of breast cancer tumors by using process of image. co occurance matrix, Laws filter, wavelet and Contourlet transform for feature extraction and for classification support vector machine was used. Cheng and Cui[12] presented fuzzy neural network (FNN) approach to detect malignant mass lesions on mammograms. Entropy, uniformity, contrast, and maximum co-occurrence are used as feature extraction. The FNN can correctly detect all malignant masses on mammograms in the testing group. A Karahaliou et al.[13] studied texture properties of the tissue surrounding MCs using a wavelet-based spatially adaptive method for mammographic contrast enhancement, followed by local thresholding to segment MCs; Four categories of textural features (first order statistics, co-occurrence matrices features, run length matrices features and Laws' texture energy measures) for texture analysis a *k*-nearest neighbor (kNN) classifier was employed for the classification of the tissue surrounding MCs, based on the extracted textural features into malignant and benign tissue. The best performance was achieved by the combined classification scheme yielding an area under the ROC curve (Az) of 0.96 (sensitivity 94.4%, specificity 80.0%). Muthu Rama Krishnan et al.[22] designed a support vector machine (SVM)-based classifier for breast cancer detection with higher degree of accuracy. They introduces a best possible training scheme of the features extracted from the mammogram, by first selecting the kernel function and then choosing a suitable training-test partition. A comparative study has been performed in respect to diagnostic measures viz., confusion matrix, sensitivity and specificity. Two different sets of data have been used taken from the Machine Learning Repository of the University of California, Irvine, USA, having nine and ten dimensional feature spaces for classification. The overall classification accuracy obtained by using the proposed classification strategy is 99.385% for dataset-I and 93.726% for dataset-II, respectively. Karthikeyan Ganesan et al.[23] presented a classification pipeline to improve the accuracy of differentiation between normal, benign, and malignant mammograms. Several features based on higher-order spectra, local binary pattern, Laws' texture energy, and discrete wavelet transform were extracted from mammograms. Feature selection techniques based on sequential forward, backward, plus-l-takeaway-r, individual, and branch-and-bound selections using the Mahalanobis distance criterion were used to rank the features and find classification accuracies for combination of several features based on the ranking. Six classifiers were used, namely, decision tree classifier, fisher classifier, linear discriminant classifier, nearest mean classifier, Parzen classifier, and support vector machine classifier. We evaluated our proposed methodology with 300 mammograms obtained from the Digital Database for Screening Mammography and 300 mammograms from the Singapore Anti-Tuberculosis Association CommHealth database. Sensitivity, specificity, and accuracy values were used to compare the performances of the classifiers. The results show that the decision tree classifier demonstrated an excellent performance compared to other classifiers with classification accuracy, sensitivity, and specificity of 91% for the Digital Database for Screening Mammography database and 96.8% for the Singapore Anti-Tuberculosis Association CommHealth database. Nabihaa Azizi et al.[24] investigated a CAD system for breast cancer by developing a novel classifier fusion scheme based fusion of three SVM classifier. Each one is associated with a homogenous family of features (Hu moments; central moments, Harelike moment) as efficient learning algorithm and diversity between features family as fusion criteria. According to the results the best accuracy of multi classifier for malignancy is 92.18% and 91.27% for benign.

In this work a technique for detecting the Brest cancer on mammogram image based on texture analysis was presented and also normal breast tissues are classified based on texture analysis.

3. MATERIAL AND METHODOLOGY

The proposed method is based on three stages: ROI selection, feature extraction, and Classification as shown in the block diagram (Fig. 1). ROIs containing the normal and abnormal tissue were processed based on texture features. These extracted features were used for classification.

3.1. Mammogram Database Formation

Digital mammograms used in this study were obtained from the Mammographic Image Analysis Society Mini-MIAS database. In this database, every image is 1024×1024 pixels and 8-bit gray level scale. It consists of 322 images which belong to normal, benign and malignant classes.[14]

On each mammogram, three regions containing the fatty, glandular and dense tissue were selected as ROIs. These three types of normal tissue were included because the classifier is developed

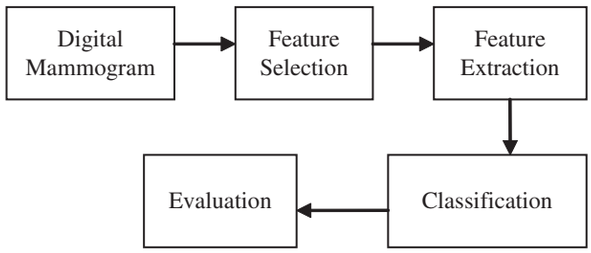

Fig. 1. Block diagram of proposed method for detection of breast cancer.

for identification of normal and abnormal tissue for all breast types. Each of these ROI_s was composed of 40×40 pixels.

3.2. Feature Extraction

Feature extraction is the techniques to measure different characteristics of image segments. Each segmented region in a scene may be described by a set of such features. In this step the features must be extracted from higher order statistical texture features.

The texture features used in this study were derived from the SGLD matrix which displays the gray level spatial dependency along different angular relationships, horizontal, vertical, right diagonal and left diagonal directions (0°, 90°, 45° and 135° respectively) and a distance d of one pixel on an image, to calculate textural measures.[15,16] The SGLD is specified by relative frequencies $P(i, j, d, \theta)$ of two pixels, separated by distance (d), along the direction of angle (θ), one with gray level i and the other with gray level j. The SGLD was calculated with window 20×20 pixels.[17] Inside each window the joint probability was calculated and then normalized by dividing the content of each element by the total content in the window, therefore the sum of the normalized matrix is equal to one.

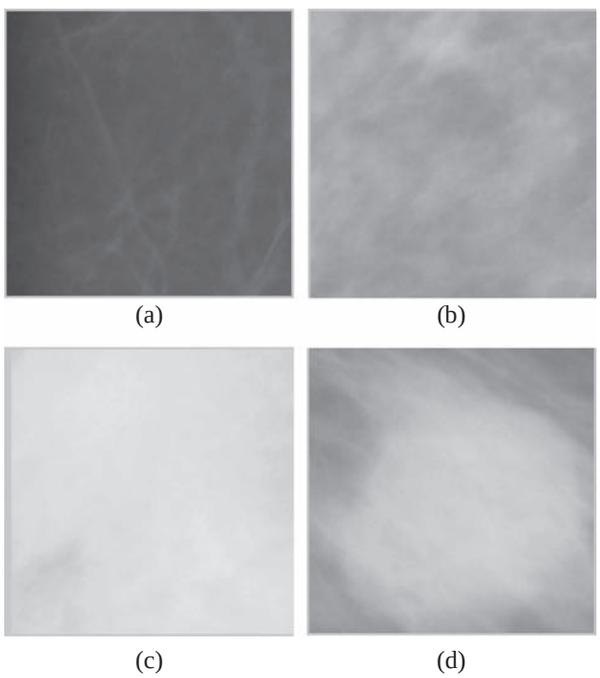

Fig. 2. Display of digital mammograms with the normal ROIs (a)–(c) (a) Fatty tissue. (b) Glandular and Connective tissue. (c) Dense tissue and (d) ROI with masses.

The non-normalized frequencies $P_{i,j}$ of SGLD matrices for a defined window $M \times N$ the distance d and angles of 0°, 90°, 45° and 135° by:

$$p(i, j, d, 0^\circ) = \#\{((k, l), (m, n)) \in (M \times N) \times (M \times N)$$
$$k - m = 0, |n - l| = d, I(k, l) = i, I(m, n) = j\} \quad (1)$$

$$p(i, j, d, 90^\circ) = \#\{((k, l), (m, n)) \in (M \times N) \times (M \times N)$$
$$|k - m| = 0, n - l = d, I(k, l) = i, I(m, n) = j\} \quad (2)$$

$$p(i, j, d, 45^\circ) = \#\{((k, l), (m, n)) \in (M \times N) \times (M \times N)$$
$$(k - m = d, n - l = -d) \text{ or } (k - m = -d, n - l = d)$$
$$I(k, l) = i, I(m, n) = j \quad (3)$$

$$p(i, j, d, 135^\circ) = \#\{((k, l), (m, n)) \in (M \times N) \times (M \times N)$$
$$(k - m = d, n - l = d) \text{ or } (k - m = -d, n - l = -d)$$
$$I(k, l) = i, I(m, n) = j\} \quad (4)$$

Where: # denotes the number of elements. It is observed that SGLD matrix is symmetrical because $P(i, j, d, \theta) = P(j, i, d, \theta)$.

Twelve texture features defined by Haralick et al.[15] were used in this study. These features were calculated from the SGLD matrix and the following equations defined these features:

(1) Entropy (EN): The Entropy coefficient (EN) is a descriptor of randomness produces a low value for an irregular SGLD matrix. It achieves its highest value when all elements of the SGLD matrix are equal for an irregular image. This coefficient is defined by the following expression:

$$EN = \sum_{i=0}^{n-1} \sum_{j=0}^{n-1} p(i, j) \log_2 p(i, j) \quad (5)$$

(2) Energy (EG): The Energy feature (EG) returns the sum of squared elements in the SGLD matrix as expressed by the following equation:

$$EG = \sum_{i=0}^{n=1} \sum_{j=0}^{n=1} p^2(i, j) \quad (6)$$

(3) Inertia (IN): The Inertia (IN) also called Contrast feature is a measure of image intensity contrast or the local variations present in an image to show the texture fineness. This parameter is specified by the following equation:

$$IN = -\sum_{i=0}^{n-1} \sum_{j=0}^{n-1} (i - j)^2 p(i, j) \quad (7)$$

(4) Inverse Difference Moment (IDM) Inverse Difference Moment is also called the "Homogeneity." Mathematically, it can be written as:

$$IDM = \sum_{i=0}^{n-1} \sum_{j=0}^{n-1} \frac{1}{1 + (i - j)^2} p(i, j) \quad (8)$$

(5) Correlation (CO) The descriptor Correlation (CO) measures the linear dependence of gray level values in the co-occurrence matrix or describes the correlations between the rows

and columns of the co-occurrence matrix. This parameter is specified by Eq. (9):

$$CO = \frac{\sum_{i=0}^{n-1}\sum_{j=0}^{n-1}(i-\mu_x)(j-\mu_y)p(i,j)}{\sigma_x\sigma_y} \quad (9)$$

(6) Variance (VA) The Variance (VA) is a measure of variation. A variance of zero indicates that all the values are identical. A non-zero variance is always positive: A small variance indicates that the data points tend to be very close to the mean and hence to each other, while a high variance indicates that the data points are very spread out from the mean and from each other.

$$VA = \sum_{i=0}^{n-1}(i-\mu)^2 p_x(i) \quad (10)$$

(7) Sum Average (SA)

$$SA = \sum_{k=0}^{2n-2} k p_{x+y}(k) \quad (11)$$

(8) Sum Entropy (SE):

$$SE = -\sum_{k=0}^{2n-2} p_{x+y}(k)\log_2 p_{x+y}(k) \quad (12)$$

(9) Sum Variance (SV)

$$SA = \sum_{k=0}^{2n-2}(k-SA)^2 p_{x+y}(k) \quad (13)$$

(10) Difference Entropy (DE)

$$DE = -\sum_{k=0}^{n-1} p_{x-y}(k)\log_2 p_{x-y}(k) \quad (14)$$

(11) Difference Average (DA)

$$DA = \sum_{k=0}^{n-1} k p_{x-y}(k) \quad (15)$$

(12) Difference Variance (DV)

$$DV = \sum_{k=0}^{n-1}(k-DA)^2 p_{x-y}(k) \quad (16)$$

Where: n is the number of grey level in the image. μ_x and μ_y are the mean and variance of the marginal distribution $P_x(i)$ and $P_y(j)$.

$$p_x(i) = \sum_{i=0}^{n-1} p(i,j) \quad (17)$$

$$p_y(j) = \sum_{j=0}^{n-1} p(i,j) \quad (18)$$

$$k = i+j, \quad k = 0,\ldots 2n-2$$

$$p_{x+y}(k) = \sum_{i=0}^{n-1}\sum_{j=0}^{n-1} p(i,j) \quad (19)$$

$$p_{x-y}(k) = \sum_{i=0}^{n-1}\sum_{j=0}^{n-1} p(i,j) \quad (20)$$

$$k = |i-j|, \quad k = 0,\ldots n-1$$

3.3. Classification

Classification is the process of classifying the input patterns into similar classes. Three factors were considered for selection of an appropriate classifier that is classification accuracy, algorithm performance and computational resources.[18] In this step breast tissues in the mammograms were classified into four classes: fatty, glandular and connective, dense tissues and abnormal classes using linear discriminant analysis.

The Linear discriminant function is formulated by a linear combination of the feature variables as shown in (21).

$$y = b + \sum_{i=1}^{n} a_i x_i \quad (21)$$

Where: n is the number of feature variables, x_i are the values of the feature variables, x_i are coefficients, and b is constant. However a_i and b were estimated from the input data during training, so that the separation between the distributions of the discriminant scores y is a maximum of groups.[2]

The efficiency of a CAD system can be classified in four perspectives:[25]

(1) True Positive (TP), when the suspected abnormality is in fact malignant;
(2) True negative (TN), when there is no detection of abnormality in a healthy person;
(3) False positive (FP), when occurs detection of abnormality in a healthy person;
(4) False negative (FN), when there is no detection of a malignant lesion.

The performance criteria are evaluated through sensitivity and specificity. The sensitivity is the fraction of the true positive cases over the real positive cases:

$$\text{Sensitivity} = \frac{TP}{TP+FN} \quad (22)$$

High values of sensitivity imply minimal false negative detection.

The specificity of the test is the fraction of the true negative cases over the real negative cases:

$$\text{Specificity} = \frac{\text{TN}}{\text{FP}+\text{TN}} \quad (23)$$

High values of specificity imply minimal false positive detection.

3.4. Proposed Detection Method

Detection is important in selecting the suspicion regions that highly resemble masses in terms of their statistical texture values.

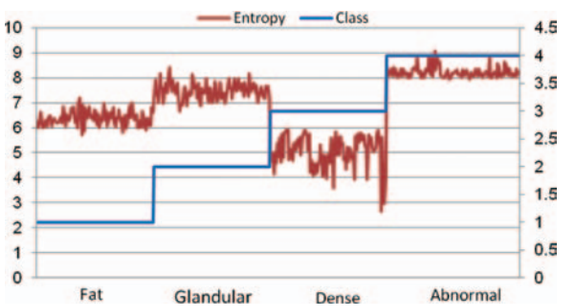

Fig. 3. Entropy variations based on tissue classeification.

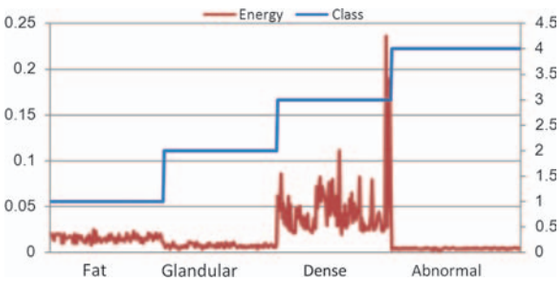

Fig. 4. Energy based on tissue classeification.

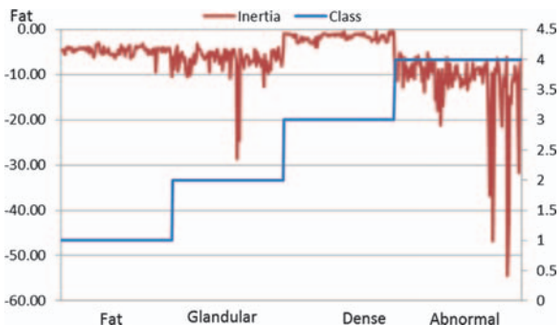

Fig. 5. Inertia based on tissue classification.

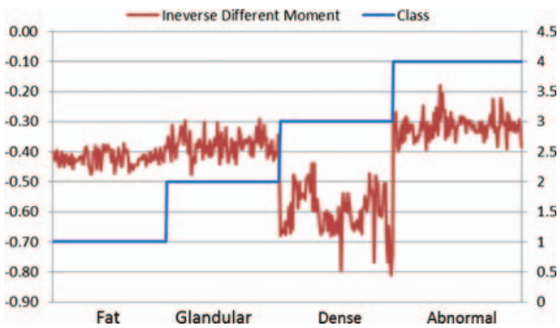

Fig. 6. Inverse different moment based on tissue classification.

The process is done based on block processing windows. Therefore, the entire ROI is divided into small window before extraction of features. In this study, detection is designed with window 20×20 pixels; at each window the features were computed.

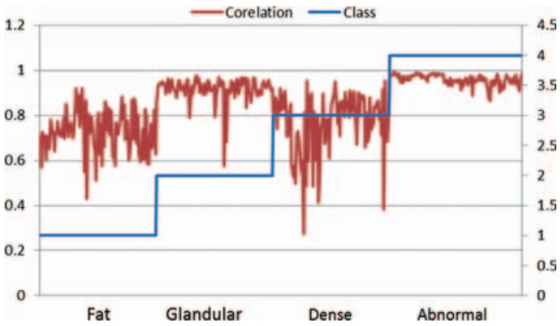

Fig. 7. Correlation based on tissue classification.

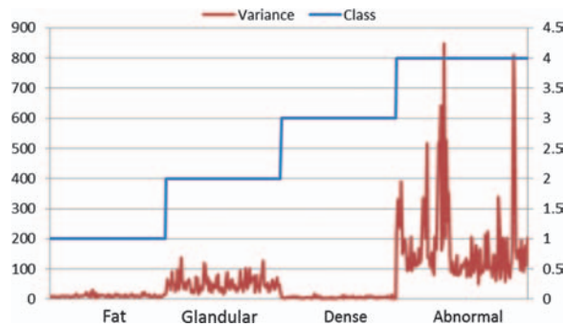

Fig. 8. Variance based on tissue classification.

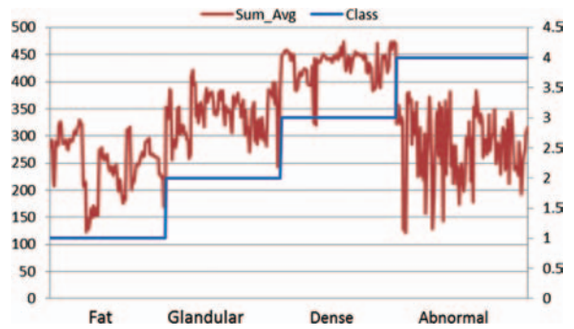

Fig. 9. Sum average based on tissue classification.

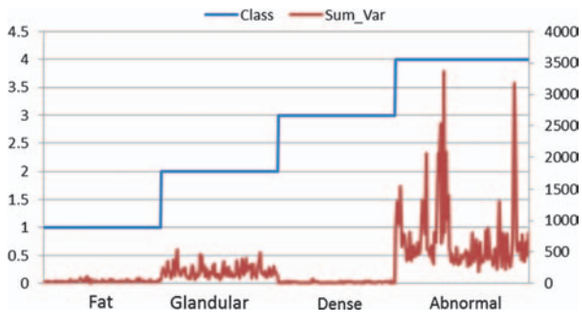

Fig. 10. Sum variance based on tissue classification.

4. RESULTS

The entire data set of 300 normal and 114 abnormal ROIs are used as input cases so that the statistical properties of the feature variables could be more reliably determined. The results of the twelve Haralick's texture features of classify the normal breast

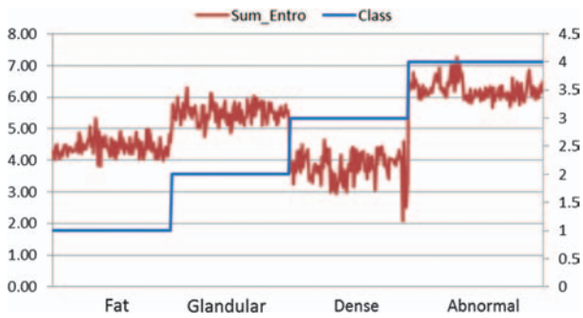

Fig. 11. Sum entropy based on tissue classification.

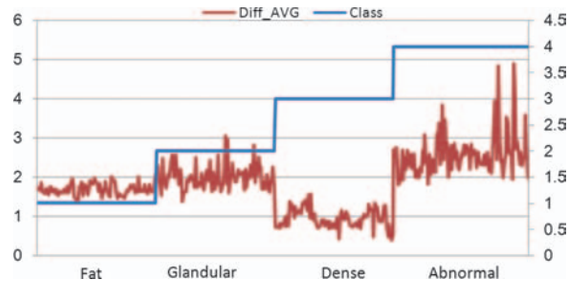

Fig. 12. Different avarage based on tissue classification.

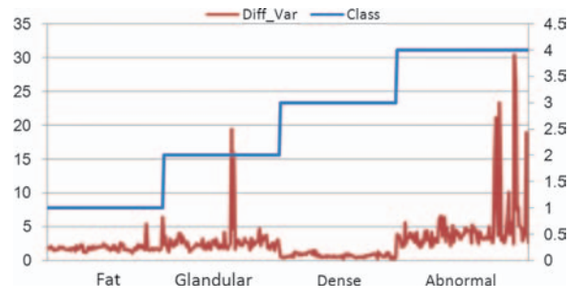

Fig. 13. Different varience based on tissue classification.

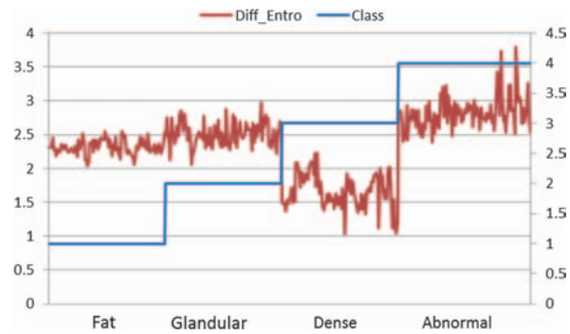

Fig. 14. Different entropy based on tissue classification.

tissue fat, (glandular and connective) and density represented in line graph by using Microsoft excel 2010 to allow for comparison between different classes; these were shown in Figures 3–14. Table I represent twelve Haralick's features of four classes are summarized into mean, standard deviation.

Table II. Normal and abnormal classification rates.

	Predicted classes (%)			
Original classes (%)	Fat	Glandular and connective	Dense	Cancer
Fat	100.0	0.0	0.0	0.0
Glandular and connective	1.0	91.0	0.0	8.0
Dense	3.0	0.0	97.0	0.0
Abnormal	0.0	5.3	0.0	94.7

Table II presents classification accuracy that was achieved by classifier. The diagonal elements indicate correct classifications, and the off-diagonal elements represent the misclassification made by the classifier. The accuracy in detecting abnormal (cancer) is 94.7%. The accuracy of the original tissue provided is 96%. The accuracy of the original classes of fat, glandular and connective and dense tissues are 100%, 91% and 97% respectively. The overall classification accuracy is 95.7% of original classes.

The performance of the classification strategy is evaluated for two classes (normal and abnormal) in Table III.

For performance evaluation, in total 414 ROIs are collected, which contains 300 normal and 114 abnormal samples. The efficacy of the classifier is realized in terms of high TP, TN, value and low FN, FP, value. The proposed feature extraction method produces 110 TP, 16 FP, 284 TN and 4 FN. The performance analysis is depicted in Table IV.

5. DISCUSSION

The stepwise disc-riminant procedure was used to select the best features. The Entropy (EN), Energy (EG), Inertia (IN), Correlation (CO), Variance (VA), Sum Average (SA), Sum Entropy (SE), Difference Entropy (DE) and Difference Variance (DV) were selected as the best features. These selected features were used to determine the coefficients of each feature variable in the discriminant function to accomplish maximum separation. The inverse difference moment (IDM) was excluded because it cannot discriminate between glandular and connective and abnormal classes (Fig. 6). The Sum Variance (SV) was excluded because it has a high deviation from its mean value in the abnormal class shown in Figure 10. Difference Average (DA) is excluded for that reason to exclude the IDM.

Observed from Table II, the best classification accuracy achieved is 100% for fatty tissue, because the fat textures were

Table I. Features statistics and its distribution over four classes.

Features	Fat	Glandular and connective tissue	Dense	Abnormal
	$\mu_1 \pm \sigma_1$	$\mu_2 \pm \sigma_2$	$\mu_3 \pm \sigma_3$	$\mu_4 \pm \sigma_4$
Entropy	6.4052 ± 0.2930	7.4937 ± 0.3345	5.0490 ± 0.6631	8.2394 ± 0.2187
Energy	0.0156 ± 0.0036	0.0073 ± 0.0018	0.0464 ± 0.0312	0.0042 ± 0.0006
Inertia	−4.7232 ± 1.0562	−6.8992 ± 3.3296	−1.6398 ± 0.7471	−11.7797 ± 7.6209
Inverse different moment	−0.4211 ± 0.0239	−0.3778 ± 0.0358	−0.6010 ± 0.0762	−0.3161 ± 0.0380
Correlation	0.7292 ± 0.0933	0.9171 ± 0.0541	0.7698 ± 0.1328	0.9588 ± 0.0240
Variance	10.8417 ± 4.2357	51.0448 ± 25.3585	5.4816 ± 2.7138	182.8855 ± 143.3777
Sum_Avg	247.8894 ± 51.2097	339.0312 ± 38.7837	432.7753 ± 28.1160	280.5164 ± 59.9386
Sum_Var	34.6435 ± 16.7261	193.2801 ± 100.8936	16.2867 ± 10.6772	715.7625 ± 569.6014
Sum_Entro	4.4310 ± 0.2812	5.4979 ± 0.2965	3.7954 ± 0.4619	6.2386 ± 0.3002
Diff_Avg	1.6833 ± 0.1423	2.0007 ± 0.3000	0.9341 ± 0.2431	2.5708 ± 0.5210
Diff_Var	1.8697 ± 0.6534	2.8074 ± 2.2552	0.7088 ± 0.2750	4.9017 ± 4.5961
Diff_Entro	2.3176 ± 0.1074	2.5138 ± 0.1734	1.6595 ± 0.2549	2.8199 ± 0.2389

Table III. Performance measures for classification.

Measures	(%)
Sensitivity (%)	96.49
Specificity (%)	94.67
Overall performance (%)	95.7

very different from the other tissues. Hence the radiologists were more confident in scoring this type of tissue. The glandular and connective tissue achieved 91% classification and 1% misclassification as fat because glandular region may contain fat tissue. May be it is difficult for the radiologist to visually distinguish the area between these tissues; therefore this caused misinterpretation in classification and 8% classified as abnormal. The classification rate of the dense tissue achieved 97% and 3% misclassification as fat. The abnormal class achieved 94.7% and 5.3% was misclassified as glandular and connective tissue.

So the proposed method in this study provides an accuracy of 95.7% for all classes in digitalized mammograms in a similar way as that of the other methods available in literature including the methods proposed by Martins et al.[7] (achieved 85% of accuracy) and Sheshadri and Kandaswamy (has obtained accuracy 78%).[6]

6. CONCLUSION

The development of CAD techniques for the detection of abnormality on mammograms may lead to efficient detection of early signs of breast cancer. The identification of normal breast tissues in mammograms is an important step in identifying abnormal tissues. This study shows the effectiveness of texture feature for classification of normal and abnormal breast tissues on digital mammograms with 95.7% relative accuracy.

References and Notes

1. H. D. Cheng, X. Cia, X. Chen, L. Hu, and X. Lou, Computer-aided detection and classification of microcalcification in mammogram: A survey. *Pattern Recognition* 36, 2967 **(2003)**.
2. H. P. Chan, D. Wei, M. A. Helvie, B. Sahiner, D. D. Adler, M. M. Goodsitt, and N. Petrick, Computer-aided classification of mammographic masses and linear discriminant analysis in texture feature space. *Phys. Med. Biol.* 40, 857 **(1995)**.
3. A. M. Sabu, D. Narain Ponraj, and Poongodi, Textural features based breast cancer detection: A survey. *Journal of Emerging Trends in Computing and Information Science* 3, 1329 **(2012)**.
4. A. M. M. Abdalla1, S. Dress2, and N. Zaki, Detection of masses in digital mammogram using second order statistics and artificial neural network. *International Journal of Computer Science and Information Technology (IJCSIT)* 3 **(2011)**.
5. T. C. Wang and N. B. Karayiannis, Detection of Microcalcifications in Digital Mammograms Using Wavelets. IEEE trans on medical imaging, University of Houston, Houston, USA **(1998)** Vol. 17, pp. 498–509.
6. H. S. Sheshadri and A. Kandaswamy, Breast tissue classification using statistical feature extraction of mammograms. *J. Medical Imaging and Information Sciences (Japan)* 23, 105 **(2006)**.
7. L. O. Martins, G. B. Junior, A. C. Silva, A. C. Paiva, and M. Gattass, Detection of masses in digital mammograms using *k*-means and support vector machine. *Electronic Letters on Computer Vision and Image Analysis* 8, 39 **(2009)**.
8. A. M. Khuzi, R. Besar, W. M. D. W. Zaki, and N. N. Ahmad, Identification of masses in digital mammogram using gray level co-occurrence matrices. *Biomed. Imaging Interv. J.* 5, e17 **(2099)**.
9. P. Gorgel, A. Sertbas, N. Kilic, O. N. Ucan, and O. Osman, Mammographic mass classification using wavelet based support vector machine, Journal Of Electrical and Electronics Engineering, Istanbul University **(2009)**, Vol. 9, pp. 867–875.
10. K. K. Rajkumar and G. Raju, A comparative study on classification of mammogram images using different wavelet transformations. International Journal of Machine Intelligence, Bioinfo Publications, USA **(2011)** Vol. 3, pp. 310–317.
11. S. Dehghani and M. A. Dezfooli, Breast cancer diagnosis system based on contourlet analysis and support vector machine. *World Applied Sciences Journal* 13, 1067 **(2011)**.
12. H. D. Cheng and M. Cui, Mass lesion detection with a fuzzy neural network. *ICASSP Cof. IEEE* 849 **(2003)**.
13. A. Karahaliou, S. Skiadopoulos, I. Boniatis, P. Sakellaropoulos, E. Likaki, G. Panayiotakis, and L. Costaridou, Texture analysis of tissue surrounding microcalcifications on mammograms for breast cancer diagnosis. *The British Journal of Radiology* 80, 648 **(2007)**.
14. Mammographic Image Analysis Society Website, http://www.wiau.man.ac.uk/services/MIAS /MIASweb.html (cited on 10/3/2013).
15. R. Haralick, K. Shanmugam, and I. Dinstein, Textural features for image classification. *IEEE Trans. Systems, Man and Cybernetics SMC-3* 610 **(1973)**.
16. S. S. S. Mole and L. Ganesan, Unsupervised hybrid classification for texture analysis using fixed and optimal window size. *(IJCSE) International Journal on Computer Science and Engineering* 02, 2910 **(2010)**.
17. F. B. Garma, M. A. Almona, M. M. Bakry, M. E. Mohamed, and A. Osman, Detection of breast cancer cells by using texture analysis. *Journal of Clinical Engineering* 38, 79 **(2013)**.
18. M. A. Jaffar1, N. Naveed, S. Zia, B. Ahmed, and T.-S. Choi, DCT features based malignancy and abnormality type detection method for mammograms. *International Journal of Innovative Computing, Information and Control* 7, 5495 **(2011)**.
19. H. Li, Y. Wang, K. J. R. Liu, S. B. Lo, and M. T. Freedman, Computerized radiographic mass detection–Part I: Lesion site selection by morphological enhancement and contextual segmentation. *IEEE Trans. Med. Imaging.* 20, 289 **(2001)**.
20. K. Ganesan, U. R. Acharya, C. K. Chua, L. C. Min, K. T. Abraham, and K. H. Ng, Computer-aided breast cancer detection using mammograms: A review. *IEEE Rev. Biomed. Eng.* 6, 77 **(2013)**.
21. H. S. Sheshadri and A. Kandaswamy, Computer aided decision system for early detection of breast cancer. *Indian J. Med. Res.* 124, 149 **(2006)**.
22. M. M. R. Krishnan, S. Banerjee, C. Chakraborty, C. Chakraborty, and K. A. Ray, Statistical analysis of mammographic features and its classification using support vector machine. *Expert Systems with Applications* 37, 470 **(2010)**.
23. K. Ganesan, U. A. 1Rajendra, K. C. Chua, C. L. Min, B. Mathew, and K. A. Thomas, Decision support system for breast cancer detection using mammograms. *Journal of Engineering in Medicine* 227, 721 **(2013)**.
24. N. Azizi, Y. Tlili-Guiassa, and N. Zemmal, A computer-aided diagnosis system for breast cancer combining features complementarily and new scheme of SVM classifiers fusion. *International Journal of Multimedia and Ubiquitous Engineering* 8, 45 **(2013)**.
25. M. Sampat, M. Markey, and A. Bovik, Computer-Aided Detection and Diagnosis in Mammography, edited by A. Bovik, Handbook of Image and Video Processing, Elsevier **(2005)**, pp. 1195–1217.

Received: 15 January 2014. Revised/Accepted: 19 March 2014.